Aggregation process on complex networks

Luis G. Morelli* and Hilda A. Cerdeira†
Abdus Salam International Center for Theoretical Physics, P.O. Box 586, 34100 Trieste, Italy
(Received 21 November 2003; published 25 May 2004)

We study the dynamics of the aggregation of particles and the evolution of the mass distribution, on a complex network which is built following the Watts-Strogatz model. The particles perform random walks following the links on the network, and aggregate when they meet other particles. On disordered networks the density of particles decays as t^{-1}, while on regular networks it decays as $t^{-1/2}$. For intermediate levels of network disorder the dynamics follows that of regular networks at intermediate density, and for low density the disorder of the network becomes relevant and the density decays as t^{-1}. The crossover time between these two regimes scales with network disorder as $t \sim p^{-2}$. We study also an annealed model for the aggregation process, in which the quenched disorder of the network is replaced by stochastic long range jumps in the particle dynamics. The annealed model is found to obey a different scaling with network disorder, with a crossover time $t \sim p^{-1}$.

DOI: 10.1103/PhysRevE.69.051107 PACS number(s): 05.40.−a, 82.20.−w, 89.75.Hc

I. INTRODUCTION

Aggregation processes are relevant to many areas of physics and chemistry, with a vast range of applications that go from stellar dynamics in astrophysics [1,2] to nucleation of droplets in vapor [3], aerosols and air pollution [4], and fractal structures grown by electrodeposition of zinc on a line electrode [5]. Also in biology and in social sciences aggregation processes have been identified in a variety of phenomena [6], where the gregarious behavior of some insects [7], cluster formation at the cellular level [8], and the growth of urban aggregates [6] are some examples. Simple models for the aggregation of particles have been studied on many different scenarios, including Euclidean and fractal spaces [9,10]. Recently, the study of natural and artificial networks has seen significative advances [11–13]. The architecture of some social and biological networks has been shown to display high clustering along with short average path lengths, and the combination of these two features has been captured by a model that interpolates between regular and random networks [11]. It is thus relevant to study how such a network architecture affects an aggregation process.

In this paper we study an aggregation process occurring on a complex network. A number of particles are placed on the nodes of the network, and they are allowed to move at random following the links to neighboring nodes. Particles aggregate when they meet, forming a new particle with the sum of their masses. The process thus defined is an irreversible coagulation reaction

$$A_i + A_j \rightarrow A_{i+j}. \tag{1}$$

We note that as far as the number of particles N is concerned, the process can be regarded as the simpler coagulation reaction

$$A + A \rightarrow A, \tag{2}$$

and the masses of the particles play no role in the dynamics. We are interested in the dynamics of this process and the structure of the mass distribution as the aggregation occurs.

The network is built according to the Watts-Strogatz (WS) model [11]. This model was introduced to describe small world phenomena and, as stated above, is an interpolation between regular and random networks. Regular networks are known to display a high degree of clustering. This is characterized by a high value of the clustering coefficient, which measures the average fraction of neighbors of a node that are in turn neighbors. Random networks, on the other hand, present very short average path lengths between nodes. The virtue of the WS model is to capture these two features, as in many instances of natural and artificial networks, where short average path lengths have been observed along with high clustering coefficients. This is the case of the *C. Elegans* neural network [11], functional networks in the human brain [14], the network defined by a power grid [11], and the network of co-authors in several databases [15], among other examples [13].

The WS network is built as follows. We start with a regular network consisting of L nodes with K links per node, with periodic boundary conditions. The nodes are arranged on a ring, and each node is connected to its K nearest neighbors to the right and to the left. We choose a node, and with probability p the link to its first neighbor in a clockwise (CW) sense is rewired to a randomly chosen node. Self-connections and repeated connections are forbidden in the model. Then we consider the next node in a CW sense and repeat the operation. We proceed with the rest of the nodes until one lap is completed. We repeat the procedure with the links to the second nearest neighbors, and so on, up to the Kth nearest neighbors. After K laps, all the links in the network have been considered once, and have been rewired with probability p to another node in the network.

Once the network has been set up, we allow one particle at each node, all particles having identical unit mass $m=1$.

*Electronic address: morelli@ictp.trieste.it
†Electronic address: cerdeira@ictp.trieste.it

The total mass in the system is thus $M=L$. The particles move as random walkers from one node to another, following the links of the underlying network. At each simulation step one particle is chosen at random and moved along a randomly chosen link to a neighboring node. If there is already a particle in the destination node, the particles aggregate and form a new particle whose mass is the sum of the masses of the colliding particles. If not, the particle simply leaves the old node and occupies the new one. The time counter is then increased in $1/N$, where N is the number of remaining particles in the system. The mass is conserved in the aggregation process, and when the aggregation is complete only one particle remains, with mass L.

In the following section, we review some known results on the dynamics of reactions (1) and (2) on Euclidean spaces, and the mean field model. In Sec. III we define the mass distribution, and some useful order parameters to describe the structure of the condensate. In Sec. IV we present the results of numerical simulations of the model, and in Sec. V we introduce the annealed model for the process and compare the numerical results with those of the quenched network model. We close in Sec. VI with a discussion of our results.

II. DYNAMICS OF THE AGGREGATION PROCESS

Mean field results for the coagulation reaction (1) have been known for a long time [16,17]. But the problem of diffusion limited coagulation on Euclidean spaces has seen further advances later in the eighties, through extensive numerical simulations [18], renormalization group theory [19], and analytical solution of the process in one dimension [20,21] among other contributions.

A natural parameter characterizing the state of the system during the aggregation process is the density $n(t)=N(t)/N(0)$, where $N(t)$ is the number of particles at time t. The mean field formulation for reaction (2) predicts an asymptotic decay for the density [17]

$$n(t) \sim t^{-1}. \tag{3}$$

Numerical simulations show that this behavior actually occurs when the space dimensionality d is larger than two, and this result was proved [19] by means of renormalization of the field theoretical description for this reaction. For $d=1$, below the critical dimensionality, it is found that [20]

$$n(t) \sim t^{-1/2}. \tag{4}$$

The effects of the initial distribution of particles were also considered [22]. The density decay described by Eq. (4) is observed after a transient, when a universal interparticle distribution is achieved. This holds as long as the initial interparticle distribution is not fractal [23].

Here, we study the coagulation reaction described by Eqs. (1) and (2) on a WS network. For $p=0$ the WS network is analogous to a one-dimensional space, where particles can make jumps of length up to K. So previous results for $d=1$ apply in this case. For $p=1$ we have a random network, analogous to a high dimensional space, and mean field results should hold. Changing the disorder parameter p we can go from regular to random networks. It is the aim of this paper to determine how this change in the network architecture affects the dynamics of the coagulation process.

In order to understand the dynamics at intermediate levels of network disorder, it is relevant to recall here some recent results [24–26] on random walks in small-world networks. It has been found [26] that the fraction of nodes visited at time t grows as

$$S(t) = t^{1/2} f(t\, p^2), \tag{5}$$

where $f(x)$ is a universal scaling function that goes to a constant value for $x \ll 1$ and grows as $\sqrt{x}$ for $x \gg 1$. These results have been also discussed in connection to the so called target problem on small world networks [25,27], a reaction of the type $A+B \rightarrow B$, where the species A is immobile.

Now, let us consider the dynamics of the aggregation process at low levels of disorder, $p \approx 0$. As the density decreases, the particles start to move without colliding. While the number of particles in the network is still high enough, they perform a random walk on a locally regular network, most of the time without traversing shortcuts, until they meet another particle. The argument of f in Eq. (5) does not grow much because p is small and t does not grow to large values before a collision occurs. So f is essentially constant and the average number of visited sites grows as $\sqrt{t}$, as in a one-dimensional system. It is only after the density becomes sufficiently low that the particles take more time to meet each other and traverse shortcuts in the process. Then the argument of f grows above 1 and $S(t) \propto t$. The dynamics of intermediate disorder networks is thus expected to follow that of regular networks in an intermediate density range, and to mimic that of disordered networks as lower densities are approached.

III. STRUCTURE OF THE CONDENSATE

In the preceding section, we have introduced the density of particles n to describe the time evolution of the process. During the aggregation process, particles of different masses are formed along the network. Although the dynamics is not sensitive to the masses of the particles in the present model, it is nevertheless interesting to study the internal structure of the condensate. In this section we introduce suitable order parameters that describe the structure of the condensate as the aggregation process takes place.

Let m denote the mass of a given particle, and N_m be the number of particles with mass m. Then we define the distribution

$$\rho(m,t) \equiv \frac{m}{M} N_m(t), \tag{6}$$

where M is the total mass in the system. This distribution gives the fraction of mass in clusters of mass m at time t, and it is normalized for all times as a consequence of mass conservation. The mean value of this distribution,

$$\langle m \rangle \equiv \sum_{m=1}^{M} m\rho(m,t), \tag{7}$$

plays an important role in the description of the process as we shall see. We also introduce an order parameter defined as the fraction of the total mass that belongs to clusters of mass $m>1$,

$$s(t) \equiv \sum_{m=2}^{M} \rho(m,t). \tag{8}$$

If we think of the particles as divided in two phases, one including the unit mass particles and the other including the condensed $m>1$ particles, then this quantity is a measure of the size of the condensate. Alternatively, we can think of $n_1=1-s$ as the fraction of remaining particles of unit mass. Note that $s=1$ does not mean complete aggregation, but simply states that there are no longer particles of unit mass.

Another quantity of interest in the aggregation process is the total number of particles—clusters—with $m>1$, which we call C. When the aggregation process begins, the value of C increases as particles aggregate and s grows. But as complete aggregation is approached, the number of particles must decrease to 1. Thus, the time evolution of C is expected to display a nonmonotonic behavior and a maximum at intermediate times. The number of clusters C can be related to the size of the condensate and the mean value of the mass distribution through some approximations. Suppose that the aggregation process occurs in such a way that the condensed particles have all the same mass μ. This equal size clusters (ESC) hypothesis has been put forward in the context of coupled oscillators [28]. Within this approximation, the mean value $\langle m \rangle$ can be written as

$$\langle m \rangle = \frac{N_1}{M} + \frac{\mu^2 C_o}{M}, \tag{9}$$

where $\mu>1$ is the mass of the clusters and $N_\mu=C_o$. The total mass in the condensate can be written as $\mu C_o=sM$, and making use of the identity $n_1+s=1$ we get for the number of clusters

$$C_o = \frac{s^2 M}{\langle m \rangle + s - 1}. \tag{10}$$

We shall test the ESC hypothesis in the following section, comparing Eq. (10) with direct calculation of C in numerical simulations.

IV. NUMERICAL SIMULATIONS OF THE MODEL

We have performed extensive numerical simulations of the system. The data presented here corresponds to $L=10^6$ networks, with $K=3$ connectivity, unless noted otherwise. In networks with $p>10^{-3}$, averages have been performed over 10^3 independent realizations. For smaller values of disorder, averages have been done over 10^2 realizations.

In Fig. 1 we show the time evolution of the density, for several values of the network disorder p, as indicated in the legend. In a finite discrete system as the one we are studying,

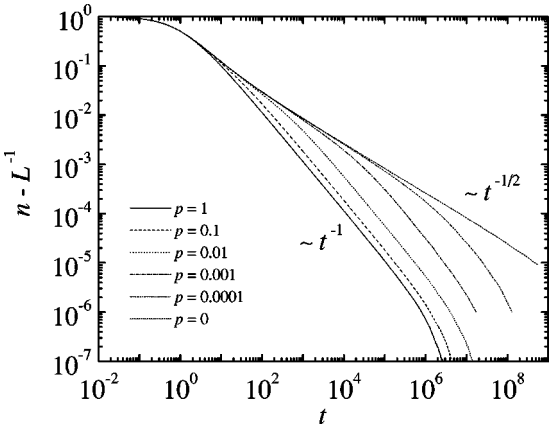

FIG. 1. Numerical results for the time evolution of the reduced density $n-L^{-1}$. The curves correspond to different levels of disorder of the network, as indicated in the key. For random and regular networks, we recover the well-known results described by Eqs. (3) and (4). For intermediate values of p, the curve follows the regular behavior in the first stage of the process, and then random network behavior as lower densities are approached.

the value of the density decays up to a minimum L^{-1}. Thus we plot, on the vertical axis, $n-L^{-1}$ to take care of this. Note that the scale is logarithmic on both axis. The well-known results for the mean field model and for the one-dimensional chain are recovered in the limiting cases $p=1$ and $p=0$. For intermediate values of p the curves are similar to the disordered case. As p becomes smaller though, the density behaves for some time as it does for regular networks, before entering the disordered regime, as it was argued at the end of Sec. II.

In the WS model, the average distance between nodes having rewired links is proportional to $1/p$ [29]. The number of visited sites grows as $\sqrt{t}$ on regular lattices. So the first shortcut is traversed by a random walker, on average, when $\sqrt{t}\sim 1/p$. The crossover observed between the regular and random regimes should occur when $p^2\ t\sim 1$. This defines the natural time scale for the process [25]. In Fig. 2 we plot $p^{-1}n$ vs p^2t, showing the data collapse for different values of disorder p. The density is scaled according to the scaling form

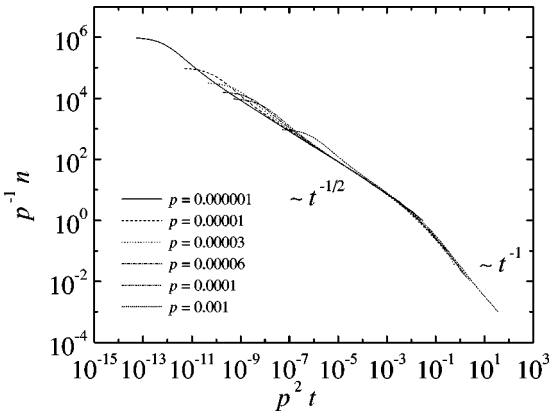

FIG. 2. Data collapse for the density decay for different levels of network disorder as indicated in the legend. The time is scaled as p^2t and the density as n/p.

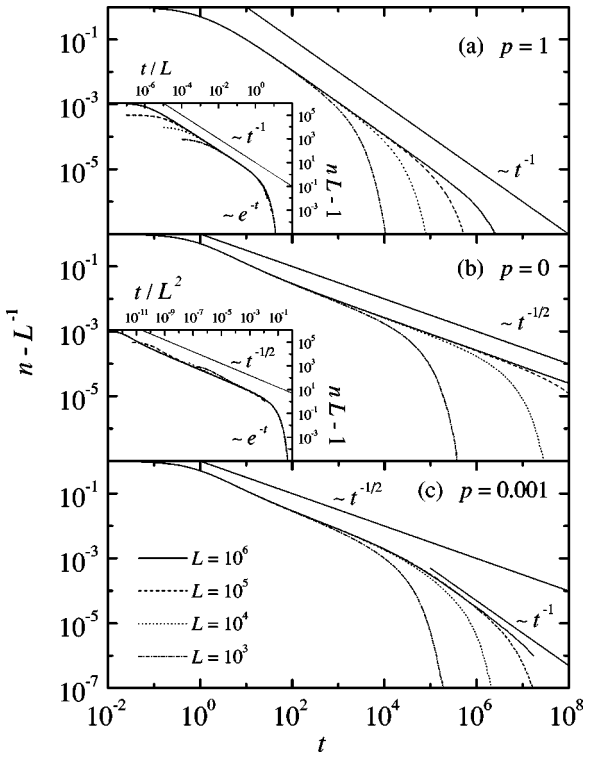

FIG. 3. Finite size effects in the density decay. The plots correspond to different levels of disorder, as indicated in each graph. The different curves in each plot correspond to different system sizes. Convergence to the different asymptotic regimes is observed as system size increases. In the inset of (a) and (b) we plot the finite size scaling for disordered and regular networks, respectively.

$$n(t) = p\psi(p^2 t), \tag{11}$$

where the scaling function $\psi(x)$ satisfies the asymptotic conditions

$$\psi(x) \sim \begin{cases} x^{-1/2} & \text{if} \quad x \ll 1, \\ x^{-1} & \text{if} \quad x \gg 1. \end{cases} \tag{12}$$

Note that deviations of the asymptotic scaling form occur for $t \to 0$, because of the uniform initial particle distribution.

In order to address the finite size effects on the dynamics we plot, in Fig. 3, the time evolution of the reduced density for different levels of disorder in the network: (a) $p=1$, (b) $p=0$, and (c) $p=0.001$. The curves in each plot correspond to different system sizes, namely, $L=10^3$, 10^4, 10^5, and 10^6. The asymptotic regimes for the density decay are observed as L grows. An exponential cutoff due to finite size effects is observed in all cases, although for $p=0$ and large system sizes it is not shown for reasons of scale. For networks with intermediate level of disorder, the different regimes can be appreciated only for large system sizes. In the case of $p=0.001$, we see clearly that for small networks the finite size effects become important before the disordered regime is reached.

In the inset of Figs. 3(a) and 3(b) we plot the finite size scaling for $p=1$ and $p=0$, respectively. In disordered networks, the average number of visited sites grows as t. Finite size effects show when $t \sim L$, defining a natural time scale tL^{-1}. In regular networks, on the other hand, the time taken by a random walker to explore the whole network grows as L^2. Finite size effects become important after this, so tL^{-2} is the time scale for the data collapse. In both cases, the reduced density is scaled as $(n - L^{-1})L$. We do not show a finite size scaling for $p=0.001$, as we have not found an appropriate scaling for this data. Just before submitting this paper we learnt of a very recent work [30], concerning the scaling properties of random walks in small-world networks, where it has been argued that scaling collapse is obtained only when the average number of shortcuts, pL, is kept constant. We have tried this scaling in our results, but we have not obtained a good collapse, maybe because the values of p were not low enough. Yet, it seems to us that the finite size scaling of random walks and diffusion limited reactions in small-world networks is not fully understood, and further study is needed to clarify this point.

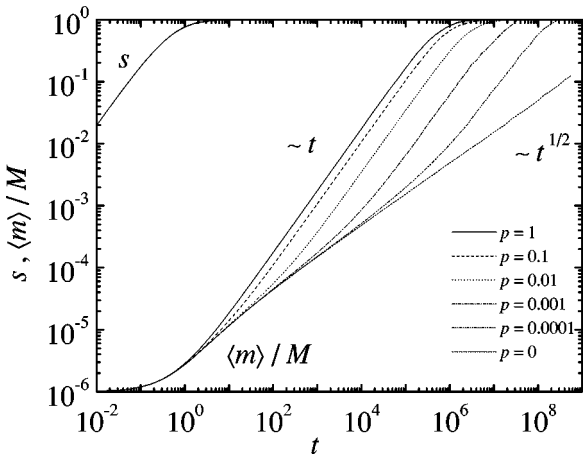

FIG. 4. Plot of the size of the condensed phase s and the normalized mean mass $\langle m \rangle / M$ as a function of time. The curves of $s(t)$ for different values of p collapse in this scale, but the time evolution of $\langle m \rangle$ shows remarkable differences as a function of network disorder p. Weakly disordered networks display a $t^{1/2}$ regime before entering the linear behavior.

Figure 4 shows the time evolution of the size of the condensed phase s and the normalized mean value of the mass distribution $\langle m \rangle / M$. The number of clusters in the system is plotted as a function of time in Fig. 5. The limit cases are again in agreement with previous results, both for the mean field model and the one-dimensional case. The curves of $s(t)$ for the different values of p collapse in this scale. All the particles go rapidly into the condensed phase as a consequence of the unit density initial condition. But to complete the condensation process takes more time. The curves of $\langle m \rangle / M$ vs t show how the coagulation takes place for different levels of disorder. For intermediate levels of disorder the mean mass grows as $t^{1/2}$ at the first stage of the process. After the characteristic time $t \sim p^{-2}$, the mean mass enters the disordered regime and grows as t. In Fig. 5, full lines correspond to direct measurements, and dotted lines to the ESC calculation. The number of clusters grow linearly with time in the first stage of the process. Then it reaches a maximum and starts to decrease. The prediction of the ESC approximation is good in the first stage of the process, but then it fails

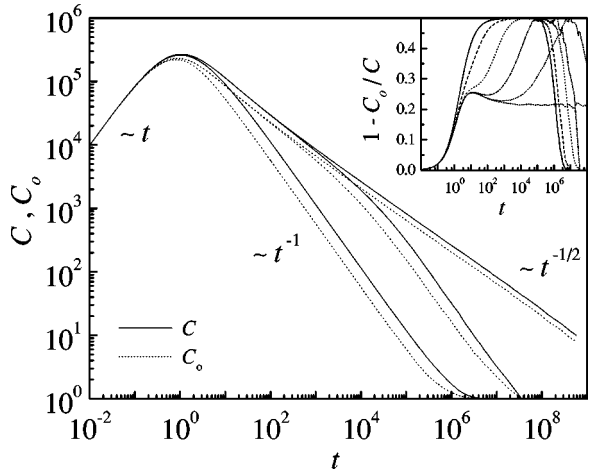

FIG. 5. Full lines stand for the time evolution of the number of clusters C and dotted lines for the ESC prediction C_o. From left to right, the curves correspond to $p=1$, 0.001, and 0. In the inset we plot $1-C_o/C$ vs t for different values of p. The relative difference between C and C_o grows up to $1/2$, due to the broadening in the mass distribution. See Fig. 4 legend for line type labels.

underestimating the number of clusters for all levels of disorder in the network. This underestimation is actually important, as it is shown in the inset of Fig. 5, where we plot $1-C_o/C$ vs t. We see that the relative difference grows up to values as high as $1/2$. This means that the mass distribution is broad and not peaked as in the ESC approximation, resulting in a larger number of clusters than predicted.

The time evolution of the mass distribution, $\rho_m(t)$, is plotted in Fig. 6 for some selected masses: $m=1$, 2, 4, 10, and 50. The fraction of mass in particles of unit mass $\rho_1(t)$ decreases monotonically, while the fraction of mass in condensed particles grows up to a maximum and then decreases. For disordered networks [Fig. 6(a)] we find that $\rho_m(t)\sim t^{-2}$ as $t\to\infty$, in agreement with the mean field result [17]. In regular networks though [Fig. 6(b)], $\rho_m(t)\sim t^{-3/2}$ in the asymptotic regime [18]. For $p=0.001$ [Fig. 6(c)], the time spanned by the scale of the graph falls entirely on the regular network regime, before crossing to the disordered network regime. This is the reason for the observed $t^{-3/2}$ decay.

Figure 7 presents some snapshots of the mass distribution $\rho_t(m)$ at different stages of the process. The time interval spanned by the snapshots for $p=1$ goes up to $t\approx 2\times 10^3$. For $p=0$ and $p=0.001$, the time interval goes up to $t\approx 3\times 10^4$. In all cases, the last snapshot corresponds to a density $n\approx 10^{-3}$. Figure 7(a) shows the distribution for disordered networks. We find that at intermediate times the distribution is linear in m for small mass values and decays as an exponential for large masses. As the asymptotic regime is reached the linear behavior extends over the whole distribution, with a peak at $m=L$. For regular networks we find a quite different situation [Fig. 7(b)], as for small mass values the distribution is quadratic. Note that a linear growth $\rho(m,t)\sim m$ implies that $N_m\sim 1$, while $\rho(m,t)\sim m^2$ implies that $N_m\sim m$. The mass distribution for $p=0.001$ networks [Fig. 7(c)] resembles the mass distribution of regular networks [Fig. 7(b)]. Indeed, for this system size and the times considered, the system is in the regular regime, as can be seen in Fig. 3.

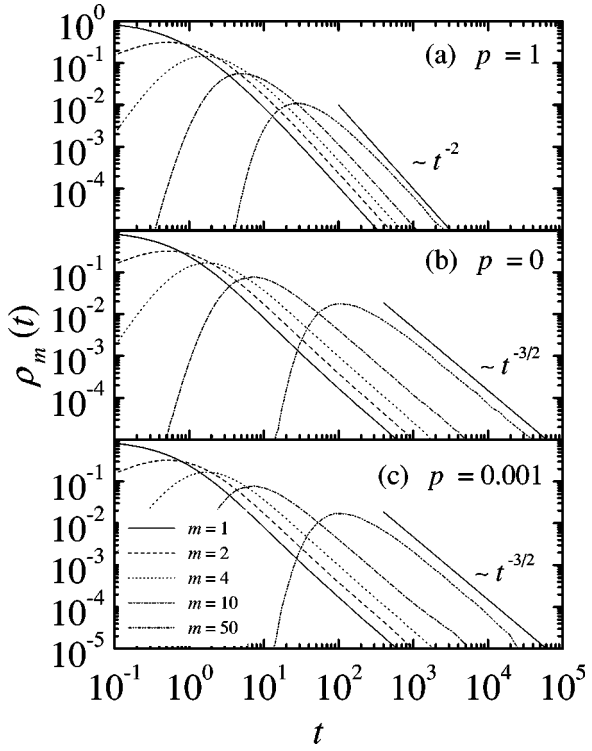

FIG. 6. Time evolution of the distribution $\rho_m(t)$ for selected values of the particle mass m, as indicated. Note carefully that for the time spanned in this scale the $p=0.001$ networks are close to the regular network regime (Fig. 1).

V. ANNEALED MODEL FOR THE AGGREGATION PROCESS

In this section we present an annealed model for the aggregation process on a WS network. The use of annealed models has proven very useful in the understanding of several problems, as random spreading in small-world networks [31], the dynamics of rumor propagation [32], and activity propagation in a system of mobile elements [33].

The annealed model replaces the quenched disorder of the network by a stochastic process. The particles move on a regular network with periodic boundary conditions. At each time step, a particle is chosen at random. With probability $(1-p)$, the particle moves to one of its $2K$ nearest neighbors in the regular network. With complementary probability p, the particle makes a long range jump to a site chosen randomly among the L nodes of the network. The aggregation process is defined as before.

In Figs. 8(a) and 8(b) we compare numerical results of the annealed model with the quenched network model, for networks with $p=1$ and $p=0.001$, respectively. Continuous lines stand for the quenched model and dotted lines for the annealed model. Averages have been done over 10^2 realizations. The qualitative aspects of both models are similar, with the same regimes in the density decay. However, the annealed model presents a faster particle density decay, and this deviation is larger for $p=0.001$ than for $p=1$. Note that we do not show results for regular networks, since both models coincide when $p=0$.

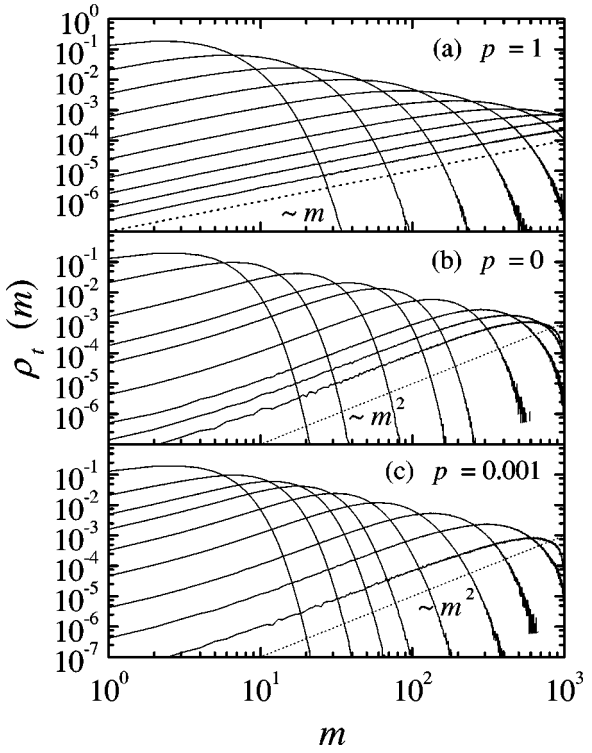

FIG. 7. Snapshots of the mass distribution $\rho_t(m)$ at different times. These simulations were done on networks of $L=10^3$ nodes, averaging over 10^7 realizations. See the text for details on the times in which the snapshots were taken. As shown by the dotted lines, for $p=1$ the distribution is linear at low mass values, while for $p=0$ it is quadratic.

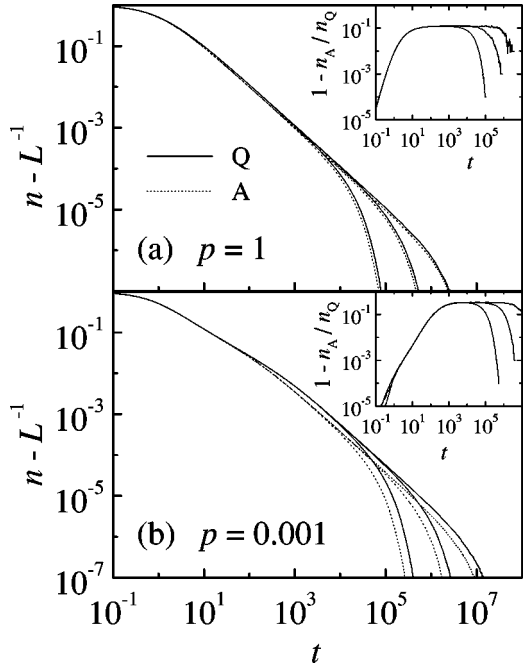

FIG. 8. Numerical results of the density decay in the annealed and the quenched network models, for disordered networks with (a) $p=1$, and (b) $p=0.001$. The curves correspond to networks of different sizes, from left to right: $L=10^4$, 10^5, and 10^6. Continuous lines stand for the quenched model and dotted lines for the annealed model. The inset shows the relative difference between the models for the same data.

In the insets of Figs. 8(a) and 8(b), we plot the relative difference $1-n_A/n_Q$ vs time, where n_A and n_Q stand for the density in the annealed and the quenched models, respectively. The difference grows up to an almost constant value, and then goes to zero when aggregation is complete in both models. Remarkably, this constant value is independent of L, for sufficiently large systems. The difference between the annealed model and the quenched model results does not diminish as $L\to\infty$.

In the annealed model, when a particle makes a long range jump to another region of the network, the probability to jump back to the node where it came from is very low. This is because the long range link is not actually there, but random long range jumps are directed to randomly chosen nodes each time they occur. In the quenched network model, however, when a particle traverses a rewired link towards another region of the network, there is always a relatively high probability for it to come back to where it came from, following the same link in the reversed direction. This is reflected in the different scaling of the two models with network disorder, as we show below.

The probability to make a long range jump, at each time step, is p. On average, the first jump is made when $pt\sim 1$. This defines, for the annealed model, a time scale and the crossover time between the regular and random regimes. In Fig. 9 we plot the scaled density $p^{-1/2}n$ vs scaled time pt, for different values of p indicated in the graph. The density is found to obey a scaling form

$$n(t) = p^{1/2}\ \psi_A(pt), \tag{13}$$

where the scaling function $\psi_A(x)$ satisfies

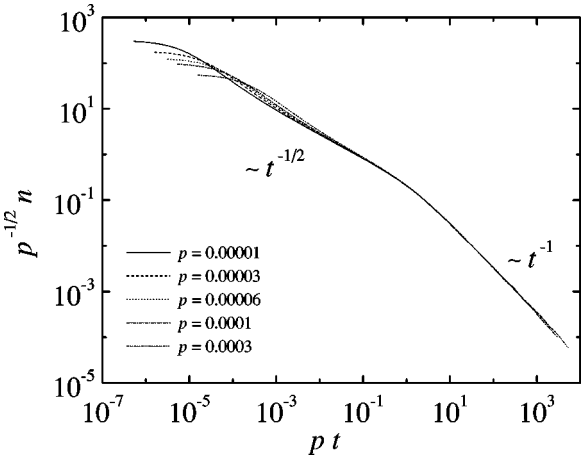

FIG. 9. Data collapse of the density decay in the annealed model. Simulations were performed on $L=10^6$ networks, averaging over 10^2 realizations. The crossover from the $t^{-1/2}$ to the t^{-1} regime occurs when $pt\sim 1$. Note the difference with the quenched network model, Fig. 2.

$$\psi_A(x) \sim \begin{cases} x^{-1/2} & \text{if} \quad x \ll 1, \\ x^{-1} & \text{if} \quad x \gg 1. \end{cases} \tag{14}$$

The characteristic time for the crossover between the regular and the disordered regimes is $t \sim p^{-1}$, in contrast with the result obtained for the quenched model (11), where $t \sim p^{-2}$.

VI. SUMMARY AND DISCUSSION

We have defined an aggregation process on a complex network, built according to the Watts-Strogatz model [11]. Unit mass particles are distributed uniformly on the nodes of the network, with unit density. The particles move on the network following the links, and aggregate when they meet. We have studied the dynamics of this process. Asymptotically, the density of particles decays as t^{-1} in the disordered network, as mean field model predicts, while on regular networks it decays as $t^{-1/2}$. For intermediate levels of disorder we find that $n \sim t^{-1}$ as $n \to 0$, but $n \sim t^{-1/2}$ at intermediate values of the density. This happens at low levels of network disorder and for large system sizes. When the density is still high enough, the particles usually meet before traversing shortcuts. But as the density gets smaller particles walk the network for longer times and traverse shortcuts before meeting, so the disordered structure of the network becomes important in the dynamics. This is reflected in the scaling form (11), which holds in the asymptotic time limit for large system sizes.

We have also studied the structure of the condensate as the aggregation takes place. Due to the dense initial condition the particles aggregate rapidly in clusters of $m > 1$. We study the time evolution of the mean mass $\langle m \rangle$ as a rough measure of the behavior of the mass distribution. The mean mass grows as $t^{1/2}$ in regular networks, and it has a linear growth in disordered networks. We have also seen that the number of clusters C grows linearly at the first stage of the aggregation process, again due to the dense initial condition. After achieving a maximum, C decays following a power law as $t^{-1/2}$ in regular networks and t^{-1} in random networks. In order to understand the evolution of the condensate we have studied the time evolution of the mass density for some values of the mass, $\rho_m(t)$. To complete the picture of the evolution of the condensate we have measured the mass distribution at different times, $\rho_t(m)$.

Finally, we have considered an annealed model for the aggregation process, in which the disorder of the network is replaced by a stochastic process in the dynamics. Particles move on a regular network, making long range jumps with probability p. The annealed model behaves similarly to the quenched network model. But the two models have different time scales and do not coincide when $L \to \infty$.

Here we have studied a simple aggregation process. The probability of aggregation when two particles meet is equal to 1, and the masses of the particles do not affect the dynamics. As an extension to the model, it should be relevant to consider the effects of the masses on the dynamics. Heavy particles could have a smaller diffusion coefficient and larger cross section than light particles. While in the present model these effects are taken to balance [18], it could be interesting to see how the dynamics changes when they do not, for different network architectures. It should also be interesting to consider reversible reactions, where it is possible for a cluster of large mass m to split into clusters of masses m_1 and m_2 such that $m = m_1 + m_2$. Finally, the analytical solution for the present simple model could be attempted as an extension of the approaches developed in Ref. [20] or in Ref. [22].

ACKNOWLEDGMENTS

The authors thank G. Abramson and D. H. Zanette for enlightening discussions and valuable suggestions.

[1] S. Chandrasekhar, Astrophys. J. **94**, 511 (1941).
[2] S. Chandrasekhar, *Principles of Stellar Dynamics* (University of Chicago, Chicago, 1942).
[3] J. Schmelzer, G. Ropke, and R. Mahnke, *Aggregation Phenomena in Complex Systems* (Wiley-VCH, New York, 1999).
[4] S. K. Friedlander, *Smoke, Dust, and Haze* (John Wiley, New York, 1977).
[5] M. Matsushita, Y. Hayakawa, and Y. Sawada, Phys. Rev. A **32**, 3814 (1985).
[6] F. Schweitzer, *Brownian Agents and Active Particles* (Springer, Berlin, 2003).
[7] H. Gruler and A. d. Boisfleury-Chevance, J. Phys. I **4**, 1085 (1994).
[8] J. L. Deneubourg, J. C. Gregoire, and E. Le Fort, J. Insect Behav. **3/2**, 169 (1990).
[9] P. A. Alemany, D. H. Zanette, and H. S. Wio, Phys. Rev. E **50**, 3646 (1994).
[10] P. Meakin and H. E. Stanley, J. Phys. A **17**, L173 (1984).
[11] D. J. Watts and S. H. Strogatz, Nature (London) **393**, 440 (1998).
[12] M. E. J. Newman, J. Stat. Phys. **101**, 819 (2000).
[13] R. Albert and A.-L. Barabási, Rev. Mod. Phys. **74**, 47 (2002).
[14] V. M. Eguíluz, D. R. Chialvo, G. Cecchi, M. Baliki, and A. V. Apkarian, e-print cond-mat/0309092.
[15] M. E. J. Newman, Proc. Natl. Acad. Sci. U.S.A. **98**, 404 (2001).
[16] M. v. Smoluchowski, Phys. Z. **17**, 557 (1916).
[17] S. Chandrasekhar, Rev. Mod. Phys. **15**, 1 (1943).
[18] K. Kang and S. Redner, Phys. Rev. A **30**, 2833 (1984).
[19] L. Peliti, J. Phys. A **19**, L365 (1986).
[20] J. L. Spouge, Phys. Rev. Lett. **60**, 871 (1988).
[21] J. L. Spouge, J. Phys. A **21**, 4183 (1988).
[22] C. R. Doering and D. ben-Avraham, Phys. Rev. A **38**, 3035 (1988).
[23] P. A. Alemany and D. H. Zanette, Chaos, Solitons Fractals **6**, 11 (1995).
[24] S. A. Pandit and R. E. Amritkar, Phys. Rev. E **63**, 041104 (2001).

[25] F. Jasch and A. Blumen, Phys. Rev. E **63**, 041108 (2001).
[26] J. Lahtinen, J. Kertész, and K. Kaski, Phys. Rev. E **64**, 057105 (2001).
[27] F. Jasch and A. Blumen, J. Chem. Phys. **117**, 2474 (2002).
[28] D. H. Zanette and A. S. Mikhailov, Phys. Rev. E **57**, 276 (1998).
[29] M. E. J. Newman and D. J. Watts, Phys. Rev. E **60**, 7332 (1999).
[30] E. Almaas, R. V. Kulkarni, and D. Stroud, Phys. Rev. E **68**, 056105 (2003).
[31] J. Lahtinen, J. Kertész, and K. Kaski, Physica A **311**, 571 (2002).
[32] D. H. Zanette, Phys. Rev. E **65**, 041908 (2002).
[33] S. C. Manrubia, J. Delgado, and B. Luque, Europhys. Lett. **53**, 693 (2001).